

A model predicting transient responses of proton exchange membrane fuel cells

J.C. Amphlett, R.F. Mann, B.A. Peppley, P.R. Roberge, A. Rodrigues

Royal Military College of Canada, Kingston, Ont. K7K 5L0, Canada

Abstract

There has been a recent interest in modelling the transient behaviour of proton exchange membrane (PEM) fuel cells. In the past, there have been several electrochemical models which predicted the steady-state behaviour of fuel cells by estimating the equilibrium cell voltage for a particular set of operating conditions. These operating conditions included reactant gas concentrations and pressures, and operating current. Steady-state behaviour is very common and in some cases is considered as the normal operating standard. Unsteady-state behaviour, however, is becoming more of an issue, especially for the transportation applications of fuel cells where the operating conditions will normally change with time. For example, system start-up, system shut-down, and large changes in the power level may be accompanied by changes in the stack temperature, as well as changes in the reactant gas concentrations at the electrode surface. Therefore, both mass and heat transfer transient features must be incorporated into an electrochemical model to form an overall model predicting transient responses by the stack. A thermal model for a Ballard Mark V 35-cell 5 kW PEM fuel cell stack has been developed by performing mass and energy balances on the stack. The thermal characterization of the stack included determining the changes in the sensible heat of the anode, cathode, and water circulation streams, the theoretical energy release due to the reaction, the electrical energy produced by the fuel cell, and the heat loss from the surface of the stack. This thermal model was coupled to a previously-developed electrochemical model linking the power produced by the stack and the stack temperature to the amount and method of heat removal from the stack. This electrochemical model calculates the power output of a PEM fuel cell stack through the prediction of the cell voltage as a complex function of operating current, stack temperature, hydrogen and oxygen gas flowrates and partial pressures. Initially, a steady-state overall dynamic model (electrochemical model coupled with the thermal model) was developed. This was then transformed into a transient model which predicts fuel cell performance in terms of cell voltage output and heat losses as a function of time due to various changes imposed on the system.

Keywords: Proton exchange membrane fuel cells; Cell voltage; Heat losses

1. Introduction

The Ballard Mark V 5 kW stack used in this study consists of 35 proton exchange membrane (PEM) fuel cells stacked in series. The fuel cells consist of a DuPont Nafion™ 117 proton exchange membrane embedded with a platinum catalyst and with an active cell area of 232 cm². The stack weighs approximately 45 kg and measures approximately 78 cm × 21 cm × 21 cm, including the active stack with the internal humidification section and cooling cells [1]. A schematic of the Ballard Mark V stack [2] is shown in Fig. 1. The series of experimental runs performed on the stack were done with air and hydrogen (although the model has been developed to deal with a reformat gas feed containing, mainly, hydrogen and carbon dioxide). Extra dry hydrogen from compressed gas cylinders and dry purified air from an air compressor enter the stack separately and are transported directly to the

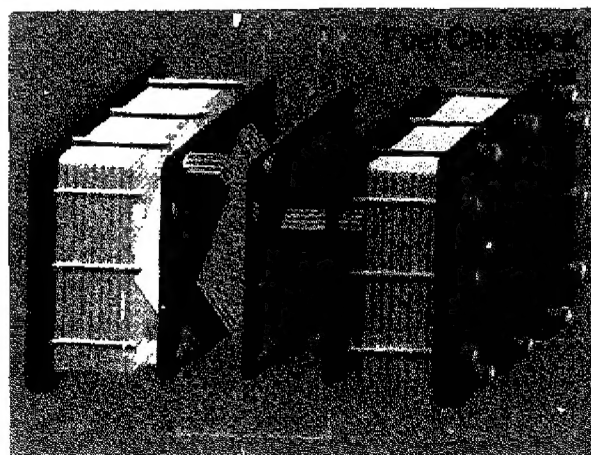


Fig. 1. Schematic of the Ballard Mark V PEM fuel cell stack [2]: (1) graphite flow field plates; (2) hydrogen gas supplied to the anode; (3) membrane electrode assembly; (4) air supplied to the cathode, and (5) single fuel cell.

humidification section where the streams pick up water vapour and are then individually fed into each of the fuel cells in their respective anode and cathode channels in the active fuel cell section. A circulating liquid water stream keeps the stack humidified and is used to control the stack temperature.

2. Steady-state electrochemical model

A steady-state electrochemical model predicting the voltage output of a Ballard Mark V 35-cell stack was previously developed by our group [3–5]. The fuel cell voltage was defined as the sum of three terms: the thermodynamic potential, E , the activation overvoltage, η_{act} , and the ohmic overvoltage, η_{ohmic} :

$$V_{cell} = E + \eta_{act} + \eta_{ohmic}$$

where

$$\eta_{act} = \xi_1 + \xi_2 T_{stack} + \xi_3 T_{stack} \ln(c_{O_2}^*) + \xi_4 T_{stack} \ln(i)$$

and

$$\eta_{ohmic} = -iR^{int} = -i(\xi_5 + \xi_6 T_{stack} + \xi_7 i) \quad (1)$$

where T_{stack} is the stack temperature (K), i is the operating current (A), $c_{O_2}^*$ is the concentration of oxygen at the catalyst interface (mol/cm³), and the ξ 's represent parametric coefficients based on experimental data which can vary in value from stack to stack. The parametric coefficients ξ_1 to ξ_4 in the activation overvoltage term, η_{act} , are based on theoretical equations from kinetic, thermodynamic, and electrochemistry fundamentals. The parametric coefficients ξ_5 to ξ_7 in the internal resistance term, R_{int} , are purely empirical based on temperature and current experimental data. A set of coefficients for the Ballard Mark V stack used in this study is shown in Table 1.

The effects of mass transport are incorporated into several of the three terms in Eq. (1). The thermodynamic potential is a function of the stack temperature, and the partial pressures of oxygen and hydrogen at the catalyst interface. The activation overvoltage is a function of the stack temperature, the operating current, and the oxygen concentration at the catalyst interface.

Table 1

List of parametric coefficients for the Ballard Mark V 5 kW stack

Coefficient	Estimate for the activation overvoltage term	Estimate for the internal resistance term
ξ_1	-0.944	
ξ_2	3.54×10^{-3}	
ξ_3	7.80×10^{-3}	
ξ_4	-1.96×10^{-4}	
ξ_5		3.30×10^{-3}
ξ_6		-7.55×10^{-6}
ξ_7		1.10×10^{-6}

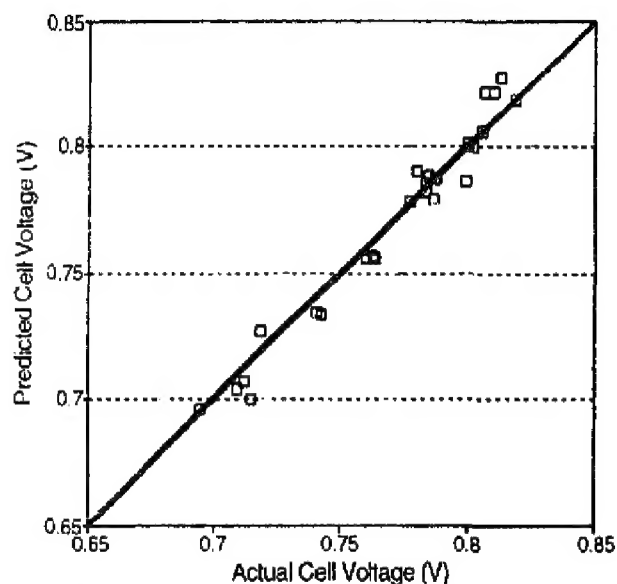


Fig. 2. Parity plot of the model-predicted cell voltage vs. the average experimental cell voltage of the Ballard Mark V 5 kW fuel cell stack.

Fig. 2 shows a parity plot of the model-predicted experimental cell voltage versus the experimental average cell voltage. It shows the validation of the steady-state electrochemical model using the coefficients in Table 1.

3. Steady-state thermal model

Mass and energy balances around the fuel cell stack were performed to calculate the various energy terms associated with fuel cell operation:

$$\dot{q}_{thcn} = \dot{q}_{scns} + \dot{q}_{elec} + \dot{q}_{loss} \quad (2)$$

The energy terms include the sensible heat calculations for each of the fuel cell streams (anode, cathode, and water), the theoretical energy produced by the fuel cell reaction, the electrical energy output, and the heat loss from the surface of the stack. These equations are defined in Fig. 3 with symbols defined in the List of symbols. Fig. 4 shows a schematic of the inlet and outlet streams in a fuel cell system, including the humidification section, identifying various parameters including flowrates from Eqs. (3)–(9) and energy terms from Eqs. (10)–(16).

Flowrates:

$$\dot{N}_{H_2,prod} = \dot{N}_{H_2,cons} = \dot{N}_{H_2,out} - \dot{N}_{H_2,in} \quad (3)$$

$$\dot{N}_{w,g,a,hum} = \left(\dot{N}_{H_2,a,in} + \dot{N}_{CO_2,a,in} \right) \left(\frac{x_{w,a}^{sat} p_{w,a}^{sat}}{p_{a,in} - x_{w,a}^{sat}} \right) \quad (4)$$

$$\dot{N}_{w,g,c,hum} = \left(\dot{N}_{O_2,c,in} + \dot{N}_{N_2,c,in} \right) \left(\frac{x_{w,c}^{sat} p_{w,c}^{sat}}{p_{c,in} - x_{w,c}^{sat}} \right) \quad (5)$$

$$\dot{N}_{w,g,a,out} = \left(\dot{N}_{H_2,a,out} + \dot{N}_{CO_2,a,out} \right) \left(\frac{x_{w,a}^{sat} p_{w,a}^{sat}}{p_{a,in} - x_{w,a}^{sat}} \right) \quad (6)$$

$$\dot{N}_{w,g,c,out} = \left(\dot{N}_{O_2,c,out} + \dot{N}_{N_2,c,out} \right) \left(\frac{x_{w,c}^{sat} p_{w,c}^{sat}}{p_{c,in} - x_{w,c}^{sat}} \right) \quad (7)$$

$$\dot{N}_{w,out} = \dot{N}_{w,in} - \dot{N}_{w,g,a,hum} - \dot{N}_{w,g,c,hum} \quad (8)$$

$$\dot{N}_{w,e,out} = \dot{N}_{w,g,a,hum} + \dot{N}_{w,g,c,hum} + \dot{N}_{H_2,prod} - \dot{N}_{w,g,a,out} - \dot{N}_{w,g,c,out} \quad (9)$$

Energy Terms:

$$\dot{q}_{theo} = \dot{q}_{rxn} = \dot{N}_{H_2,cons} \Delta H_{R,T} \quad (10)$$

$$\dot{q}_{elec} = n V_{cell} i \quad (11)$$

$$\dot{q}_{sens,a} = \dot{N}_{H_2,a,out} \hat{c}_{p,H_2} (T_{a,out} - T_o) + \dot{N}_{CO_2,a,out} \hat{c}_{p,CO_2} (T_{a,out} - T_o) + \dot{N}_{w,g,a,out} H_{w,g} \\ - \dot{N}_{H_2,a,in} \hat{c}_{p,H_2} (T_{a,in} - T_o) - \dot{N}_{CO_2,a,in} \hat{c}_{p,CO_2} (T_{a,in} - T_o) \quad (12)$$

$$\dot{q}_{sens,c} = \dot{N}_{O_2,c,out} \hat{c}_{p,O_2} (T_{c,out} - T_o) + \dot{N}_{N_2,c,out} \hat{c}_{p,N_2} (T_{c,out} - T_o) + \dot{N}_{w,g,c,out} H_{w,g} \\ - \dot{N}_{O_2,c,in} \hat{c}_{p,O_2} (T_{c,in} - T_o) - \dot{N}_{N_2,c,in} \hat{c}_{p,N_2} (T_{c,in} - T_o) \quad (13)$$

$$\dot{q}_{sens,w} = \dot{N}_{w,out} \hat{c}_{p,w} (T_{w,out} - T_o) - \dot{N}_{w,in} \hat{c}_{p,w} (T_{w,in} - T_o) \quad (14)$$

$$\dot{q}_{sens} = \dot{q}_{sens,a} + \dot{q}_{sens,c} + \dot{q}_{sens,w} \quad (15)$$

$$\dot{q}_{loss} = \dot{q}_{theo} - \dot{q}_{elec} - \dot{q}_{sens} \quad (16)$$

Fig. 3. Thermal analysis equations for the Ballard Mark V 5 kW stack.

The average heat transfer coefficient for the stack may be estimated using the average heat loss from the surface of the fuel cell stack:

$$(hA)_{stack} = \frac{\dot{q}_{loss}}{(T_{stack} - T_{room})} \quad (17)$$

Experimental values of heat loss were obtained from the Ballard Mark V fuel cell data to yield an average $(hA)_{stack}$ of 17 W/K.

For comparison, the predicted heat loss by natural convection can be estimated using the Nusselt equation [6]:

$$h = \frac{k}{L} a (Gr \cdot Pr)^m \quad (18)$$

where a and m are numerical parameters which are found in Ref. [6]. Note that the Nusselt equation includes the Grashof, Gr , and Prandtl, Pr , numbers.

Our calculated values for h from this natural convection correlation range from about 3 to 7 W/(m² K) for stack temperature from about 25 to 85 °C, corresponding to $(hA)_{stack}$ values from about 1 to 2 W/K. The present exper-

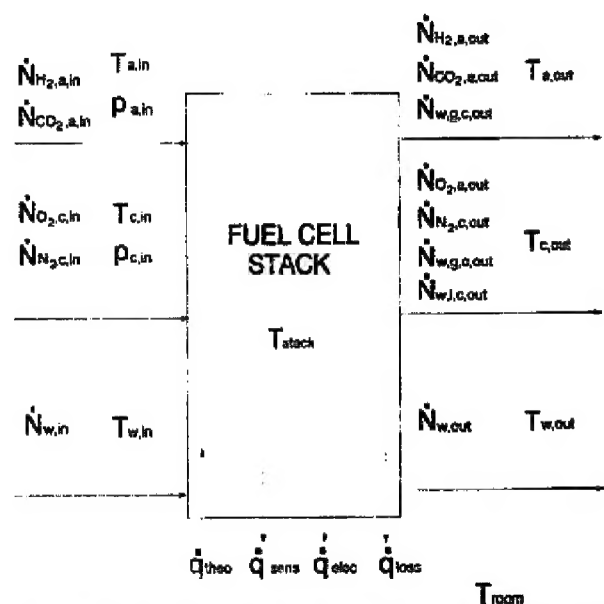


Fig. 4. Schematic of the inlet and outlet streams in a fuel cell system identifying various parameters including flowrates and energy terms defined in Fig. 3.

Table 2
Heat transfer parameters for the Ballard Mark V fuel cell stack

Heat transfer parameter	Approximate value (W/K)
$(hA)_a$	2
$(hA)_c$	10
$(hA)_w$	50
$(hA)_{stack}$	17

imental $(hA)_{stack}$ values in the 10 to 20 W/K range are clearly higher than those expected from natural convection alone. Welty et al. [6] quote approximate h ranges from 5 to 50 W/(m² K) for natural convection of air and 25 to 250 W/(m² K) for forced convection of air. For further comparison, Fuller and Newman [7] and Nguyen and White [8] proposed h values for fuel cell heat losses to air in the range of 25 to 26 W/(m² K) for gases in forced convection which correspond to $(hA)_{stack}$ values in the range of 7 to 10 W/K, again lower than our experimental values.

Possible explanations for the apparent disagreements could be the presence of conduction losses from the stack to the bench and from the stack up the heavy copper power cables, plus forced circulation of laboratory air which results in heat transfer further up the forced convection scale than assumed in the publications cited above [7,8]. The mean (hA) value of 17 W/K for our particular stack and experimental configuration is considered quite acceptable. This value may then be used in Eq. (17) to predict the heat loss from the stack at various stack temperatures.

Similarly, the increase in sensible heat terms can also be linked to heat transfer coefficients, $(hA)_i$, from the stack to the fluid, i , where i = anode, cathode, or water stream, using:

$$\begin{aligned}
 (hA)_a &= \frac{\dot{q}_{sens,a}}{T_{stack} - 0.5(T_{a,in} + T_{a,out})} (hA)_c \\
 &= \frac{\dot{q}_{sens,c}}{T_{stack} - 0.5(T_{c,in} + T_{c,out})} (hA)_w \\
 &= \frac{\dot{q}_{sens,w} + \dot{q}_{hum}}{T_{stack} - 0.5(T_{w,in} + T_{w,out})}
 \end{aligned} \quad (19)$$

The heat transfer parameters, $(hA)_i$, as shown in Table 2 were approximated based on preliminary data obtained from the Ballard Mark V stack. Note that the heat transfer parameter for the stack is also shown in the Table for completeness.

Table 3 shows a typical application of the steady-state thermal model at an operating current of 20 A. The last column shows the actual experimental data at the same operating conditions. Generally, the model predicts the experimental data very well.

4. Transient model

A model predicting transient responses in fuel cell operation was developed based on coupling the steady-state elec-

trochemical model with an unsteady-state thermal model to form an overall transient model. Initially an overall steady-state model was developed to describe the steady-state equilibrium conditions of the fuel cell and then the model evolved into an overall transient model describing fuel cell characteristics as a function of time until a new steady-state is reached.

An unsteady-state energy balance is the extension of the steady-state thermal model by the addition of an accumulation term, such that:

$$MC \left(\frac{dT_{stack}}{dt} \right) = \dot{q}_{theo} - \dot{q}_{elec} - \dot{q}_{sens} - \dot{q}_{loss} \quad (20)$$

where M is the total mass of the fuel cell stack, C is the average specific heat of the stack, and dT_{stack}/dt is the temperature change with respect to time.

The estimated value of MC in the accumulation term may be determined by using the summed $M_i C_i$ values of the individual components of the fuel cell stack such as the graphite and stainless steel. The masses of the individual components were calculated based on the average density of the material, and the specific heats were estimated from data in the literature. A value for the sum of $M_i C_i$ was estimated as 35 kJ/K. The MC value may also be measured using an experimental approach by rearranging Eq. (20):

$$MC = \frac{\dot{q}_{theo,f} - \dot{q}_{elec,f} - \dot{q}_{sens,f} - \dot{q}_{loss,f}}{\left(\frac{dT_{stack}}{dt} \right)_i} \quad (21)$$

where the subscript i represents values immediately after a step change in power and the subscript f represents the 'final' values following a step change in power. An average value for MC was calculated as approximately 35 kJ/K which agrees with the previous MC calculation.

The transient model may be obtained by coupling the steady-state electrochemical model and the thermal model as a function of time with the new accumulation term from Eq. (20) giving:

$$\frac{dT_{stack}}{dt} = \frac{1}{MC} (\dot{q}_{theo} - \dot{q}_{elec} - \dot{q}_{sens} - \dot{q}_{loss}) \quad (22)$$

with all the terms on the right side of the equation defined and quantified earlier. This expression can then be used as a basis of a finite-element calculation using:

$$T_{stack,j+1} = T_{stack,j} + \left(\frac{dT_{stack}}{dt} \right)_j \Delta t \quad (23)$$

with a Δt value appropriate to the stack, approximately one minute or less for this study. The steady-state electrochemical model imports a current value of T_{stack} along with the other required system parameters and then provides a V_{cell} for the calculation of the updated value of \dot{q}_{elec} . The thermal model calculates the new outlet stream temperatures based on the current value of T_{stack} so that the \dot{q}_{sens} term may be calculated. The remaining energy terms, \dot{q}_{theo} and, \dot{q}_{loss} are dependent on T_{stack} . A new value for dT_{stack}/dt is then calculated using

Table 3

Typical application of the steady-state thermal model when a load of 20 A is applied to the fuel cell system

Model input data			Model output data			
Stream	Parameter	Value	Stream	Parameter	Predicted value	Experimental value
Inlet anode gas	$N_{H_2, \text{in}}$	0.0078 mol/s	Outlet anode gas	$N_{H_2, \text{out}}$	0.0041 mol/s	0.0041 mol/s
	$T_{a, \text{in}}$	23.5 °C		$T_{a, \text{out}}$	28.5 °C	25.3 °C
	$P_{a, \text{in}}$	35 psig				
Inlet cathode gas	$N_{O_2, \text{in}}$	0.004 mol/s	Outlet cathode gas	$N_{O_2, \text{out}}$	0.0022 mol/s	0.002 mol/s
	$T_{c, \text{in}}$	23.5 °C		$T_{c, \text{out}}$	40.0 °C	38.8 °C
	$P_{c, \text{in}}$	35 psig				
Inlet water	$N_{w, \text{in}}$	1.84 mol/s	Outlet water	$T_{w, \text{out}}$	31.7 °C	23.9 °C
	$T_{w, \text{in}}$	23.5 °C				
Other data	T_{room}	23.5 °C	Other data	T_{stack}	40.0 °C	38.0 °C
	k_{cells}	35 cells		V_{cell}	0.825 V	0.817 V
	i	20 A		V_{stack}	28.9 V	28.6 V
				P_{stack}	578 W	572 W

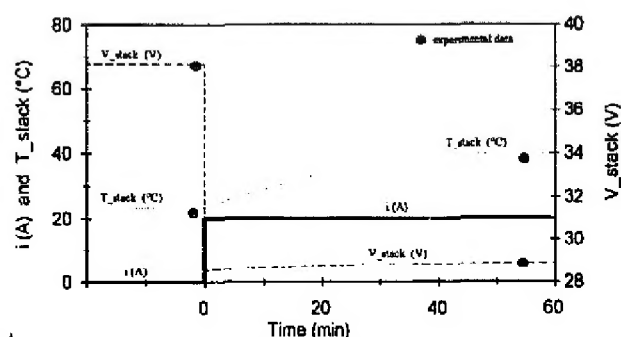


Fig. 5. Transient plot for the start-up of the Ballard Mark V stack from 0 to 20 A.

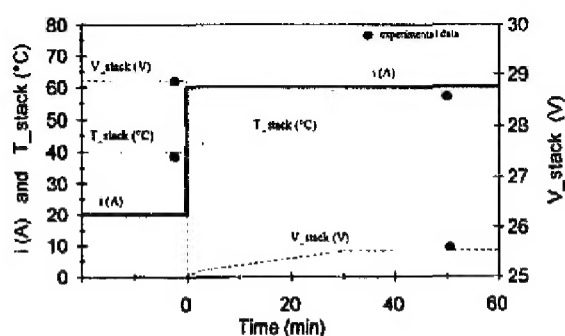


Fig. 6. Transient plot for the 'load step-up' of the Ballard Mark V stack from 20 to 60 A.

Eq. (22) so that a new T_{stack} for the next time step may be calculated using Eq. (23). As a result, the transient model calculates T_{stack} and the outlet stream temperatures, V_{cell} , and ultimately the power P as a function of time.

Fig. 5 shows the application of the transient model for the start-up of the fuel cell stack for an operating current from 0 to 20 A. Fig. 6 shows the power step-up from 20 to 60 A and Fig. 7 shows the shut-down of the fuel cell stack from 60 to 0 A. Each of the three plots also show some experimental data for reference. In general, the transient model predicts the experimental data very well.

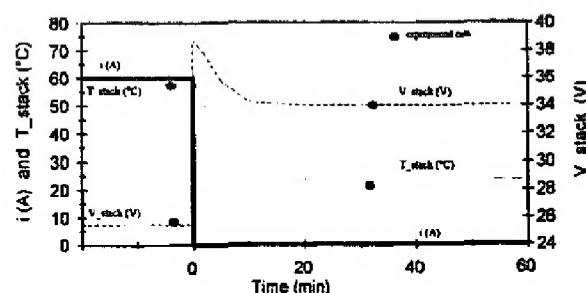


Fig. 7. Transient plot for the shut-down of the Ballard Mark V stack from 60 to 0 A.

5. Conclusions

The transient model is a useful tool in predicting the performance of the PEM fuel cell stack in our experimental configuration. For example, given a set of gas feed conditions, pressures, heat transfer coefficients, and operating current, the model will lead to a unique solution for stack voltage, stack power, and stack temperature. If the stack undergoes a perturbation, such as the initial start-up, a large step in current, or a shut-down, the transient model will be able to generate transient information such as stack temperature, cell voltage, and power as a function of time.

The steady-state electrochemical model parameters, the heat capacity, and the heat transfer coefficients are obviously specific to the stack used and to the immediate surroundings of the stack. These values would have to be recalculated for another fuel cell stack system. The general methodology, however, should be applicable to any PEM stack system.

6. List of symbols

α	constant in the Nusselt equation
A	surface area, m^2
c	concentration, mol/cm^3

C	average heat capacity, J/(kg K)
E	thermodynamic potential, V
E^0	standard electrochemical energy, V
F	Faraday's constant, $F=96\,487\text{ C/equivalent}$
Gr	Grashof number
h	convective heat transfer coefficient, $\text{W}/(\text{m}^2\text{ K})$
H	change in enthalpy, J/mol
i	operating current, A
I	current density, A/ft^2 or ASF
k	thermal conductivity, $\text{W}/(\text{s m K})$
M	mass of the fuel cell, kg
m	constant in the Nusselt equation
N	molar flowrate, mol/s
n	number of cells in the stack
P	power output, W
PEM	proton exchange membrane
Pr	Prandtl number
q	energy, W
R	ideal gas constant, $R=8.3145\text{ J}/(\text{mol K})=0.08206\text{ l atm}/(\text{mol K})$
R	resistance, Ω
T	temperature, K
V	output voltage, V

Greek letters

ΔH	heat of reaction, J/mol
η	overvoltage, V
ξ	parametric coefficient in the fuel cell model

Subscripts

a	anode
act	activation
c	cathode
cell	proton exchange membrane fuel cell
cons	consumed
elec	electrical
g	gas
hum	humidification
in	in

int	internal
l	liquid
loss	loss
ohmic	ohmic
out	out
prod	product
rxn	reaction
stack	fuel cell stack
sens	sensible
theo	theoretical
w	water

Superscripts

sat	saturation
*	at the catalyst interface

Acknowledgements

We would like to thank the Department of National Defence and the Chief of Research and Development for financial support.

References

- [1] D.H. Swan, B.E. Dickinson and M.P. Arikara, *Advancements in Electric and Hybrid Electric Vehicle Technology*, Society of Automotive Engineers, Warrendale, PA, USA, 1994, pp. 19–30.
- [2] Ballard Power System Inc., Annual rep., 1994, North Vancouver, BC, Canada.
- [3] J.C. Amphlett, R.M. Baumert, R.F. Mann, B.A. Peppley, P.R. Roberge and A. Rodrigues, *J. Power Sources*, **49** (1994) 349–356.
- [4] J.C. Amphlett, R.M. Baumert, R.F. Mann, B.A. Peppley, P.R. Roberge and T.J. Harris, *J. Electrochem. Soc.*, **142** (1995) 1–8.
- [5] J.C. Amphlett, R.M. Baumert, R.F. Mann, B.A. Peppley, P.R. Roberge and T.J. Harris, *J. Electrochem. Soc.*, **142** (1995) 9–15.
- [6] J.R. Welty, C.E. Wicks and R.E. Wilson, *Fundamentals of Momentum, Heat, and Mass Transfer*, Wiley, New York, 3rd edn., 1984; C.O. Bennett and J.E. Myers, *Momentum, Heat, and Mass Transfer*, McGraw-Hill, New York, 2nd edn., 1974.
- [7] T.F. Fuller and J. Newman, *J. Electrochem. Soc.*, **140** (1993) 1218–1225.
- [8] T.V. Nguyen and R.E.J. White, *J. Electrochem. Soc.*, **140**, 8 (1993) 1218–1225.